Study of turbulent wavy annular flow inside a 3.4 mm diameter vertical channel by using the Volume of Fluid method in OpenFOAM

Journal of Physics: Conference Series **2766** (2024) 012067 doi:10.1088/1742-6596/2766/1/012067

Study of turbulent wavy annular flow inside a 3.4 mm diameter vertical channel by using the Volume of Fluid method in OpenFOAM

E Zanetti[1], A Berto[2], S Bortolin[2], M Magnini[3] and D Del Col[2]

[1] Department of Process and Energy, Delft University of Technology
Leeghwaterstraat 39, 2628 CB Delft, the Netherlands
[2] Department of Industrial Engineering, University of Padova
Via Venezia 1, 35131 - Padova, Italy
[3] Department of Mechanical, Materials and Manufacturing Engineering
University of Nottingham, Nottingham, UK

E-mail: E.Zanetti@tudelft.nl

Abstract. In annular downward flow, an annular liquid film flows at the perimeter of the channel pushed down by the gravity force and by the shear stress that the vapor core exerts on it. Depending on the working conditions, the vapor-liquid interface can be flat or rippled by waves. The knowledge of the liquid film thickness is very important for the study of annular flow condensation because the thermal resistance of the liquid is often the most important parameter controlling the heat transfer. A new approach for the simulation of annular flow is here proposed using an in-house developed transient solver based on the Volume of Fluid (VOF) adiabatic solver interIsoFoam available in OpenFOAM. With the VOF method, in addition to the standard set of equations (continuity and momentum), a transport equation related to the advection of the volume fraction scalar field has to be solved. The numerical setup consists of 2D axisymmetric domain. An adaptive mesh refinement (AMR) method is added to the solver to better capture the interface position. The k-ω SST model is used for turbulence modelling in both the liquid and vapor phases and a source term (whose magnitude is controlled by a model parameter named B) is included in the ω equation to damp the turbulence at the interface.

1. Introduction

Two-phase annular flow in vertical channels is characterized by the presence of a vapor/gas core with a liquid film at the wall. This flow regime is encountered in many engineering processes and in particular it is observed during condensation/evaporation inside channels. The knowledge of the liquid film flow-dynamics, in terms of waves formation, propagation and structure is essential to understand the heat and mass transfer mechanisms governing condensation [1] or evaporation processes. CFD simulations could represent a powerful tool to take a closer look at the liquid film, especially when dealing with small diameter channels. Due to the challenges associated with the simulation of complex two-phase flows, the available studies are still limited [2,3] and validation with experiment data is needed. In the present paper, an OpenFOAM solver based on the Volume of Fluid (VOF) method and Adaptive Mesh Refinement (AMR) is developed for the simulation of vertical annular flow in a 2D-axisymmetric

domain. The solver uses the *k-ω* model for turbulence closure, with the addition of a turbulence damping model. Recent CFD studies on annular flow using the turbulence damping approach used a fixed value of the damping parameter [4] but its effect on the waves behaviour is not clear yet, even if soe investigations have been made [3]. In this work, the effect of turbulence damping on waves structures are analyzed and compared against experimental data.

2. Governing Equations

CFD simulations of downward annular flow with refrigerant R245fa inside a vertical channel have been realized with the open-source library OpenFOAM. In particular, a new transient solver has been developed starting from an existent Volume of Fluid (VOF) based adiabatic solver (*interIsoFoam*). In the VOF method, the so-called one fluid formulation is used to describe the fluid domain where, in addition to the conventional set of equations, namely continuity and momentum (eq. 1-2), a transport equation related to the advection of the "volume fraction" scalar field (α) has to be solved (eq. 3).

$$\frac{\partial \rho}{\partial t}+\nabla\cdot(\rho\bar{u})=0 \tag{1}$$

$$\frac{\partial(\rho\bar{u})}{\partial t}+\nabla\cdot(\rho\bar{u}\bar{u})=-\nabla p+\nabla\cdot\left[(\mu+\mu_t)\left(\nabla\bar{u}+\nabla\bar{u}^T\right)\right]+\bar{f_\sigma} \tag{2}$$

$$\frac{\partial \alpha}{\partial t}+\nabla\cdot(\alpha\bar{u})=0 \tag{3}$$

In the numerical implementation, the volume fraction is defined as the fraction of computational cells occupied by the liquid ($0< \alpha <1$ at the interface). Accordingly, the density and the viscosity of the two-phase mixture are calculated as:

$$\rho=\alpha\cdot\rho_l+(1-\alpha)\cdot\rho_v \tag{4}$$

$$\mu=\alpha\cdot\mu_l+(1-\alpha)\cdot\mu_v \tag{5}$$

Where the subscript *l* and *v* identify the liquid and vapour phase respectively.

In eq. 2 the term $\bar{f_\sigma}$ is associated with the surface tension and it is calculated according to Municchi et al. [5].

$$\bar{f_\sigma}=\sigma\frac{\nabla\alpha}{|\nabla\alpha|} \tag{6}$$

In the present numerical simulations, RANS (Reynolds Averaged Navier Stokes) approach is used to solve the smallest spatial-temporal scales with the objective of computational time reduction. In particular, the *k-ω* SST model has been adopted, leading to two additional transport equations to be solved, one for the turbulent kinetic energy *k* and one for the specific rate of dissipation *ω*. This turbulence model was previously found to accurately reproduce annular flow condensation of R134a in a 1 mm diameter channel [6]. However, the main drawback of the available RANS models is that they have been developed for single-phase flows and therefore they could lead to less accurate results close to the liquid-vapor interface.

Usually, in RANS-VOF models, corrections are applied to address this issue. The most popular method is that proposed by Egorov [7] which adds a source term in the *ω* equation, to damp out the turbulence at the liquid-vapor interface. The following term has been implemented, according to the modifications recently proposed by Fan and Anglart [8]:

$$S_\omega=\frac{36\cdot 2|\nabla\alpha|}{\beta y^3}B^2\left(\delta\frac{\alpha\mu_l^2}{\rho_l}+\frac{(1-\alpha)\mu_v^2}{\rho_v}\right) \tag{7}$$

In eq. 7 β is a constant of the turbulence model, y is a length scale [8] and B is the damping parameter, for whose quantification there are no guidelines provided in the literature. Finally, δ is a factor that controls the symmetry of the damping source: if δ is equal to 1 the original model from Egorov is obtained [7] and the turbulence is damped both in the liquid and vapour side of the interface, whereas if δ is < 0 the turbulence damping is treated asymmetrically, resulting in a turbulence enhancement in the liquid side. In the present paper, the results with asymmetric damping are reported:

$$\delta = -\frac{\mu_v^2}{\mu_l^2}\frac{\rho_l}{\rho_v} \tag{8}$$

This formulation ensures that when the two-phases' properties are the same, no damping is performed.

3. Numerical setup

3.1. Boundary conditions

The presented computational domain consists of a 2D axisymmetric channel, as depicted in figure 1. Simulations have been run considering a channel radius R equal to 1.7 mm and a total length of the tube equal to 40R. The tested fluid is R245fa, whose thermophysical properties are reported in table 1 for the tested conditions.

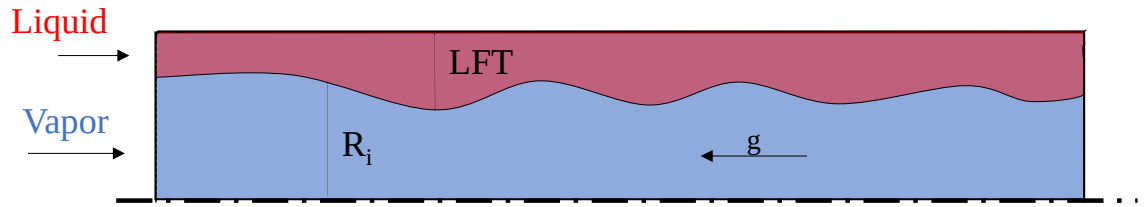

Figure 1. Sketch of the computational domain used for annular flow simulations. R_i is the radial coordinate of the liquid-vapor interface, LFT is the liquid film thickness.

Table 1. Properties of liquid and vapor R245fa in saturated conditions.

Fluid	T_{sat} **[K]**	ρ_l **[kg m^{-3}]**	ρ_v **[kg m^{-3}]**	μ_l **[Pa s]**	μ_v **[Pa s]**	σ **[N m^{-1}]**
R245fa	315.65	1289	15.16	$3.19\cdot10^{-4}$	$1.1\cdot10^{-5}$	0.014

The input for the model are the mass flux $G = \dot{m}/A_{tot}$ and the vapor quality $x = \dot{m}_v/\dot{m}$ (A_{tot} is the channel cross-section, $\dot{m}$ is the refrigerant mass flow rate). Since the velocity profile and the void fraction field (equal to one between the wall and the coordinate R_i and equal to zero between R_i and the symmetry axis) must be set as boundary conditions, the following two approaches have been used.

- A#1. Velocity profiles for both liquid and vapor phase are calculated by solving the continuity and momentum equations in the radial direction (in cylindrical coordinates) assuming steady-state laminar flow. The profile of the axial velocity u has the following form:

$$u = \frac{r^2}{4\mu}\frac{\partial p}{\partial z} + \log(R)\,C_1 + C_2 = 0 \tag{9}$$

  In eq. 11 z is the axial coordinate. The unknowns $\partial p/\partial z$, R_i and C_1, C_2 (for the two phases) are obtained by applying the following additional boundary conditions: null velocity in the radial direction, null variation of pressure along the radial direction, free-shear of the liquid at the interface and of the vapor at the symmetry axis, same velocity of the two phases at the interface and no-slip condition at the wall.
- A#2. Inlet velocities are assumed to be uniform in the liquid and vapor phase. A_v is the channel cross-section occupied by the vapor. Therefore:

$$u_v = \frac{\dot{m} \cdot x}{\rho_v A_v} = \frac{\dot{m} \cdot x}{\rho_v \pi R_i^2} \tag{10}$$

$$u_l = \frac{\dot{m}(1-x)}{\rho_l (A_{tot} - A_v)} = \frac{\dot{m}(1-x)}{\rho_l \pi (R^2 - R_i^2)} \tag{11}$$

u_v and u_l are thus obtained by providing a guess value of R_i.

3.2. Mesh design and refinement

Adaptive Mesh Refinement (AMR) has been implemented in the solver. During the simulations, the mesh is automatically refined when the volume fraction field assumes values between 0.1 and 0.9. This process occurs every five time steps. Various levels of refinement can be performed and, during each refinement operation, one cells is divided into 4 identical cells. In addition, cells close to the wall are statically refined using the same splitting method (in this case maintaining constant the number of cells during the entire simulation). The remaining part of the domain is cover with a structured meshed having square cells.

Three mesh zones can be identified: a) refined cells at the wall that cannot be unrefined; b) cells that are refined due to the passage of the liquid-vapor interface; c) unrefined cells in the vapour bulk and in the liquid film (far from the wall). Figure 2 shows the mesh configuration during a transient simulation in annular flow. The refined and unrefined cells at the interface and the wall cells are highlighted. The liquid wave in contact with the wall is depicted in red (α=1) whereas the vapour bulk is depicted in blue (α=0). After a sensitivity analysis, a mesh with unrefined cell size (UCS) equal to R/64 and 3 refinement levels both at the wall and at the interface has been adopted for the simulations.

The adoption of this mesh design allowed to reduce by 58% the number of cells compared to the reference case in which the refined cells are static and cover a region equal to the average maximum liquid film thickness. Under this configuration, the calculated y+ at the centre of the first wall cell was found to be between 0.58 and 0.85 for the presented simulations.

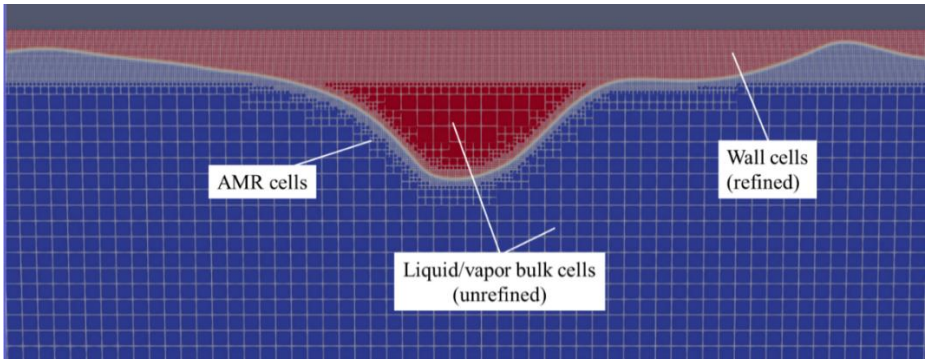

Figure 2. Structure of the mesh during the passage of a wave.

4. Results

4.1. Effect of inlet conditions

Simulations have been performed to assess the effect of the adopted inlet boundary conditions method (named A#1 and A#2) on the resulting liquid film thickness. Figure 3 reports the evolution of the time-averaged liquid film thickness along the channel axis for various inlet conditions in the case of vapor quality equal to 0.39 and mass flux G = 100 kg m^{-2} s^{-1}. In particular, simulations with the A#2 method have been run by assuming various values of R_{int} at the inlet (1UCS, 2UCS, 3UCS). In each of these tests, the thickness of the mesh layer with fixed-size and refined cells was assumed to be equal to R_{int}. It can be noted that the calculations performed with the method A#1 predict a higher LFT at the inlet of the channel. After a certain axial distance from the inlet, the predicted LFT overlap and the calculated

LFT is not dependent on the method used to set the inlet conditions. However, attention must be paid to the fact that the liquid film needs some space to develop, i.e. to reach a spatial steadiness.

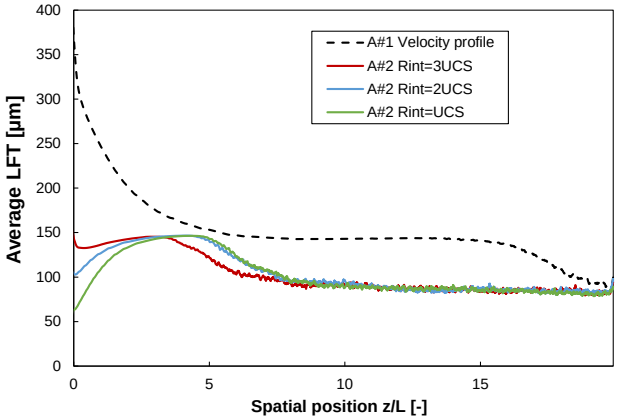

Figure 3. Computed time-averaged liquid film thickness along the channel. Results obtained with approach #1 and #2 are reported.

4.2. Effect of turbulence damping

Figure 4-left reports the values of the average liquid film thickness (LFT) obtained with the simulations conducted without turbulence damping (B=0 in eq. 7) for different values of vapor quality (from 0.39 to 0.77). Figure 4 also reports the measured LFT vales [1]. It can be observed that the model tends to underestimate the liquid film thickness by 10-30 µm and, even if this deviation is rather small compared to the size of the channel (3.4 mm), this could be relevant in relative terms. Figure 4-right reports the results of the simulations obtained with B=1. The results show that an increase in the damping parameter leads to a significant change in the average LFT, which increases by 36% - 51%.

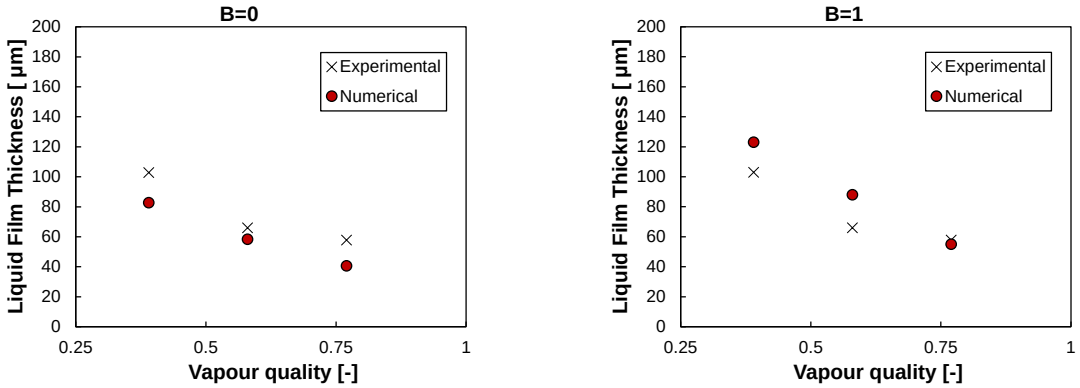

Figure 4. Comparison between computed and measured (Berto et al. [1]) time-averaged liquid film thickness for turbulence damping B=0 (left) and B=1 right. Mass flux G = 100 kg m^{-2} s^{-1}.

Turbulence damping does not only affect the time-average liquid film thickness, but it also influences waves characteristics. Reconstructed images from post-processed LFT vs time data revealed that, when no damping is applied, the liquid-vapor interface is mainly flat with the appearance of some regular disturbance waves. On the contrary, when B=1 the liquid film is characterized by higher frequency ripple waves. Figure 5 shows the frequency distribution for the LFT obtained from the numerical simulations and compared against the experiential results. The frequency distribution is obtained dividing the whole range of variation for LFT in intervals (bins) having the same size. Numerical results and experimental data are then sampled considering a frequency equal to 1000 Hz. By counting the number of events that fall within each considered bin, the graphs in Figure 5 can be realized. For vapor quality x = 0.77 and B=1 the LFT frequency distribution obtained from the simulations overlaps the experimental one.

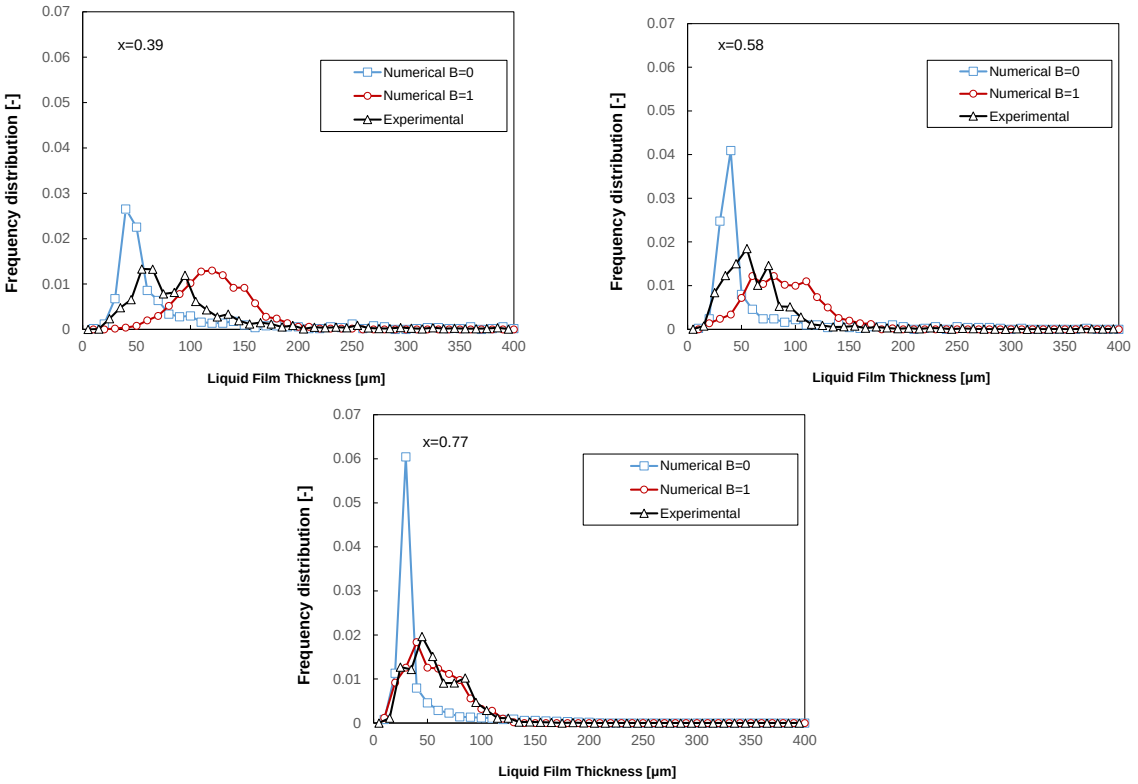

Figure 5. Calculated and measured (Berto et al. [1]) LFT frequency distributions for various vapor qualities and mass velocity G = 100 kg m^{-2} s^{-1}. The simulations are run with B=0 and B=1.

Conclusions

An OpenFOAM solver based on the VOF method has been developed to perform transient numerical simulations of annular flow with R245fa inside a 3.4 mm diameter circular channel. The numerical setup consists of a 2D axisymmetric domain with AMR applied at the interface. The results show that, for a given condition of mass velocity and inlet vapor quality, after a certain length of the channel, the calculated LFT is no longer dependent on the velocity profile assumed as boundary condition. Computed LFT values have been compared against experimental data. The introduction of a damping factor B=1 is responsible for higher computed values of the time-averaged LFT and it also changes the frequency distribution, leading to an interface characterized by higher frequency ripples. Given the asymmetric nature of the damping source term, a wider analysis on the impact of B will be conducted in the future.

References

[1] Berto A, Lavieille P, Azzolin M, Bortolin S, Miscevic M and Del Col D 2021 *International Journal of Multiphase Flow* **140** 103649
[2] Fan W, Li H and Anglart H 2019 *International Journal of Multiphase Flow* **110** 256–72
[3] Fan W, Cherdantsev A V. and Anglart H 2020 *Energy* **207** 118309
[4] Varallo N, Mereu R, Besagni G and Markides C N 2024 *Chemical Engineering Research and Design* **201** 631–44
[5] Municchi F, El Mellas I, Matar O K and Magnini M 2022 Conjugate heat transfer effects on flow boiling in microchannels *Int J Heat Mass Transf* **195**
[6] Da Riva E, Del Col D, Garimella S V. and Cavallini A 2012 *Int J Heat Mass Transf* **55** 3470–81
[7] Egorov Y, Boucker M, Martin A, Pigny S, Scheuerer M and Willemsen S 2004 *5th Euratom Framework Programme ECORA project* **2004** 91–116
[8] Fan W and Anglart H 2019 *Fluids* **4** 136